ARTICLE

Synchronized Polymerization and Fabrication of Poly(acrylic acid) and Nylon Hybrid Mats in Electrospinning

Daman Chandra Parajuli,[†] Madhab Prasad Bajgai,[†] Jung An Ko,[†] Hyo Kyoung Kang,[‡] Myung Seob Khil,[‡] and Hak Yong Kim*,[‡]

Department of Bionanosystem Engineering, College of Engineering, and Department of Textile Engineering, Chonbuk National University, Jeonju 561-756, Republic of Korea

ABSTRACT Acrylic acid monomer in a viscous supporting nylon solution was polymerized and fabricated simultaneously via an electrospinning process. This novel polymerization method defines the fiber morphology as a network of interconnected mats. This network consists of smaller poly(acrylic acid) (PAA) fibers, approximately 19 nm in diameter, and larger nylon 6 fibers, approximately 75 nm in diameter. These two different fibers are separated by extraction of PAA from the fibrous mat in water and differentiation of field-emission scanning electron microscopy (FESEM) images of the same mat using before and after extraction of PAA. The structure of the extracted PAA was confirmed by ^{1}H NMR and Fourier transform infrared (FT-IR) analysis. The observed modification to conventional electrospun mats is due to the presence of an extra phase-separated PAA produced by the electrospinning polymerization process. Finally, fiber morphologies and hybrid property were characterized via FT-IR, FESEM, thermogravimetric analysis, and X-ray diffraction. Similarly extracted samples and synthesis PAA were characterized in FT-IR and ^{1}H NMR spectroscopy.

KEYWORDS: electrospinning • polymerization • nanofiber • hybrid mat • poly(acrylica acid) • nylon 6 • morphology

INTRODUCTION

Nanoimaging technology has led to an investigation of the morphological, physical, and chemical characteristics of materials on the nanoscale. As an example, this technology allows for the capture of magnified images of electrospun fibers, giving a good representation of the morphology, texture, and geometry. This imaging technology also allows researchers to develop high-quality, durable fibers and has been extensively studied for use in nanocomposites (1, 2), biomedical applications (3−5), super hydrophobic membranes (6, 7), and sensors (8, 9). Nowadays, the 3D structure of a electrospinning fibrous mat is very important in both academic and research fields. Kim et al. worked on cellulose nanofibers (10), and Ding et al. demonstrated PAA and nylon 6 2D and 3D structures, in which they explain engineering about their great work (11). Similarly, our research concerned making an interconnected mat using nylon 6 and acrylic acid monomer and polymerizing it to form smaller netlike fibers of poly(acrylic acid) (PAA) inside the big nylon 6 fiber.

Nylon 6, also known as polycaprolactam and polyamide 6, which is a biodegradable (11) and biocompatible material, possesses excellent physical and mechanical properties and is one of the most widely used synthetic polymers for fibers. It was used in this study with an additional polymer to form hybrid fibers containing carboxylic acid groups. Carboxylic acid groups are useful for many applications including adhesion and various biotechnological applications. Carboxylic acid groups present in PAA chains allow for many types of bond formation, such as hydrogen, ionic, covalent, and coordination, and these bonding types have been used to make hydrogels (12, 13), chelating agents, esters, and complex nanoparticles (14, 15). PAA is driven from acrylic acid, which is especially useful because of its conjugated double bond and carbonyl group. These groups are important for nucleophilic and free-radical reactions for organic synthesis and polymerization processes. The chemical properties of acrylic acid allow for different polymerization processes, such as radical polymerization for commercial PAA, electropolymerization for thin-film formation (16, 17), and plasma polymerization for surface modification (18−20). This study focuses on the polymerization of acrylic acid for producing interconnected fibrous mats via electrospinning. These mats have potential applications in tissue engineering, aerospace, semipermeable membranes, and filters.

The electrospinning technique has been predominantly used for fiber production driven by electrostatic forces. By electrospinning of a selective monomer and catalyst in a viscous supporting solution, polymerization and mat fabrication can be performed simultaneously. Generally, the viscous solution containing the polymer includes functional groups on its branches and terminal ends, which can react with the substrate or monomer to initiate polymerization. Chemical reaction is only possible if one or more of the reacting substrates can be activated within the electric field. When this reaction is carried out, covalent cross-links can form

* E-mail: khy@chonbuk.ac.kr.
Received for review October 10, 2008 and accepted February 21, 2009
[†] Department of Bionanosystem Engineering, College of Engineering.
[‡] Department of Textile Engineering.
DOI: 10.1021/am800191m

Published on Web 03/18/2009

between parallel fibers and nanorods, which can be advantageous for various applications.

In electrospinning processes, a high voltage is applied across the viscous polymer solution. When this solution is sprayed through the syringe spinneret, a chemical reaction occurs and a Taylor cone (21) is formed at the tip of the pendant droplets because of electrostatic forces between the tip and the grounded collector. Above the critical voltage, electrostatic forces overcome the surface tension of the solution and an electrified polymer jet is formed (22). If these polymer jets contain a phase-separated polymer layer, the phases can still potentially interconnect into nanorods. The jet is then elongated and whipped continuously by electrostatic repulsion until it is deposited on the grounded collector in the form of a randomly interwoven cylindrical fibrous mat.

In this study, acrylic acid polymerization is achieved via formic acid reduction during the electrospinning process. Typically, formic acid loses a proton in the acrylic acid solution because of the high acidity. Deprotonated formic acid splits into CO_2 and a hydride ion, which works as a reducing agent (23−26). If the hydride ion attacks a β carbon of an α,β unsaturated carbonyl monomer (acrylic acid), group-transfer polymerization can be initiated (27−29). In the performance of polymerization via electrospinning, it is difficult to control all parameters, such as the pressure, temperature, and concentration; however, there is sufficient control to allow for the investigation of structural, chemical, and physical modifications of electrospun mats.

MATERIALS AND METHODS

Preparation of an Interconnected Fibrous Mat (Electrospinning Polymerized PAA/Nylon 6 or EPPN). A nylon solution was first prepared by nylon 6 (22 wt %) pellets, which were purchased from Kolon Co., Kwachon, South Korea, by adding in a mixture of 8 parts formic acid (99%, purchased from Showa Co., Tokyo, Japan) and 2 parts acetic acid (99%, purchaged from Showa Co., Tokyo, Japan). This solution was stirred for 24 h at room temperature. A total of 3 mL of the nylon 6 solution was transferred into a 50 mL glass vial containing 3 mL of fresh liquid acrylic acid monomer (98%, Junsei Chemical Co., Tokyo, Japan), and the resulting mixture was stirred for 5 min at room temperature. Approximately 2 mL of the nylon 6 and acrylic acid solution was isolated for electrospinning polymerization in a syringe pump fitted with a pointed nozzle, which was clamped at about a 20° angle relative to the horizontal axis. The positive pole electrode was secured inside the solution. An electric voltage was applied at 24 kV, and the electrospun fibers were deposited on a grounded, metal, rotating collector, which was positioned 12 cm from the tip of the syringe. Once the fibrous EPPN mat became thick enough, it was separated from the collector for analysis.

Extraction and Polymerization of Samples. Our aim was extraction of PAA from the EPPN mat, which was made up of nylon 6 and acrylic acid monomer, during the electrospinning process. Two pieces of mat cut from a single mat were used to extract samples A and B, respectively. One simple different process was applied before the extraction process; these two samples exhibit remarkable identification separately, which was more significant for our research. Similarly, sample C was polymerized via solution chemistry to demonstrate the effect of formic acid behind the formation of PAA.

Table 1. ^{1}H NMR Chemical Shifts of the Reference Compound and Samples

SN	name of the compound	chemical shift [^{1}H NMR (D_2O) δ][a]
1	acrylic acid	6.16 (1H, J = 18.6 Hz, d), 5.91 (1H, J = 19.8 and 13.4 Hz, dd), 5.74 (1H, J = 10.3 Hz, d), 4.14 (0.3H, J = 16.3 and 5.9 Hz, dt), 2.54 (0.3H, J = 5.9 Hz, t)
2	sample A	6.41 (1H, J = 18.1 Hz, d), 6.18 (1H, J = 17.3 and 11.0 Hz, dd), 5.96 (1H, J = 8.8 Hz, t), 4.37 (1H, J = 6.1 Hz, t), 2.91 (31H, J = 7.8 Hz, t), 2.56 (1H, J = 6.1 Hz, t), 1.76 (31H, J = 11.0 and 4.2 Hz, tt), 0.63 (31H, J = 8.5 Hz, t)
3	sample B	2.91 (1H, J = 7.8 Hz, t), 1.77 (1H, J = 927.7 Hz, t), 1.76 (1H, J = 11.2 and 4.2 Hz, tt), 0.63 (1H, J = 8.5 Hz, t)
4	sample C	2.91 (1H, J = 7.8 Hz, t), 1.76 (1H, J = 11.0 and 4.2 Hz, tt), 0.63 (1H, J = 8.5 Hz, t)

[a] Spectra of this table are shown in Figure 4.

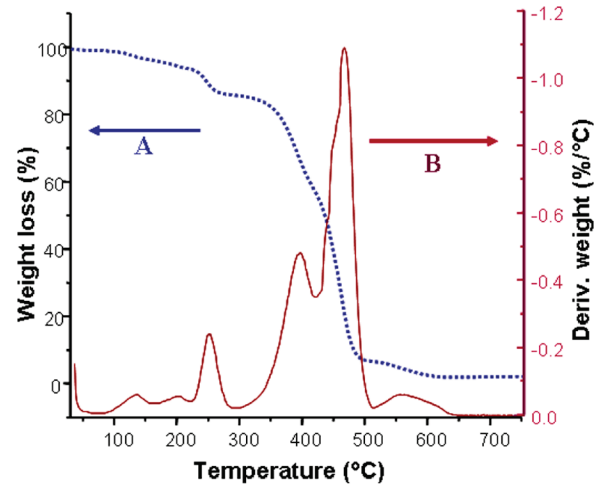

FIGURE 1. Net TGA and DTG graphs of the EPPN mat: (A) TGA; (B) DTG. Derivative: the peak temperatures are at 127, 200, 243, 382, and 459 °C.

Sample A. This sample was extracted from 80 mg of the EPPN mat, which was submersed into 100 mL of water in a 250 mL beaker. This sunken mat was shaken for 36 h at room temperature on an electric shaker. After collection of the sample in solution, the solution and mat were separated by filtration. A filtrate solution was taken, and about 85% of the solvent was evaporated by direct heating and then drying in an oven at 80 °C for 4 h. The weight of the resulting solute was obtained as 18 mg of slightly pale-yellow solid sample A. The ^{1}H NMR spectrum of this sample is described in Table 1.

Sample B. This sample was also extracted from about 80 mg of the EPPN mat. This mat was dried in an oven at 80 °C for 48 h and was then dried under vacuum for 24 h at 60 °C. After drying, the mat was submersed into 100 mL of water in a 250 mL beaker. This sunken mat was shaken for 36 h at room temperature on an electric shaker. After collection of the sample in solution, the solution and mat were separated by filtration. A solution was taken, and about 85% of the water was evaporated by direct heating and then drying in an oven at 80 °C for

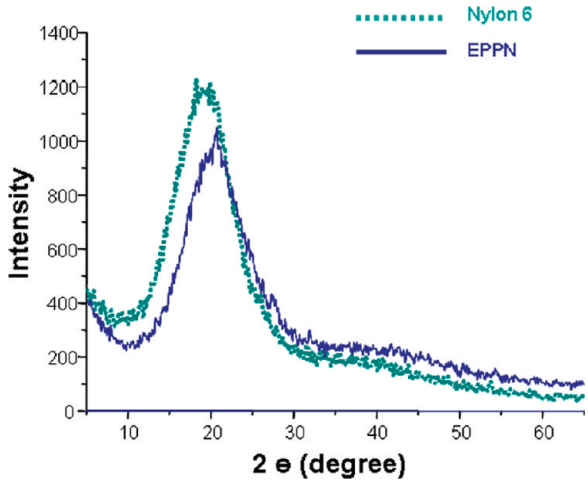

FIGURE 2. XRD patterns of nylon 6 and EPPN mats.

4 h. The weight of the resulting pale-yellow solute sample B obtained was 17 mg. The ^{1}H NMR spectrum of this sample is described in Table 1.

Sample C. Sample C was prepared by a typical PAA polymerization. A total of 5 mL of acrylic acid was transferred into a three-necked 250 mL round-bottomed flask, which was equipped with a reflux condenser and a mechanical stirrer. Formic acid (1 mL) was added to the flask, and the solution was refluxed. The reaction was stirred under reflux at 130 °C for 1.8 h. Upon completion, the solid product was wetted by submersion in water and shaking on a mechanical shaker for 48 h. The resulting viscous PAA liquid was washed with acetone and methylene chloride and then dried in a fume hood at room temperature. After becoming partially solidified, the sample was dried in an oven at 80 °C for 48 h and then dried further under vacuum for 24 h. The ^{1}H NMR spectrum of this sample is described in Table 1.

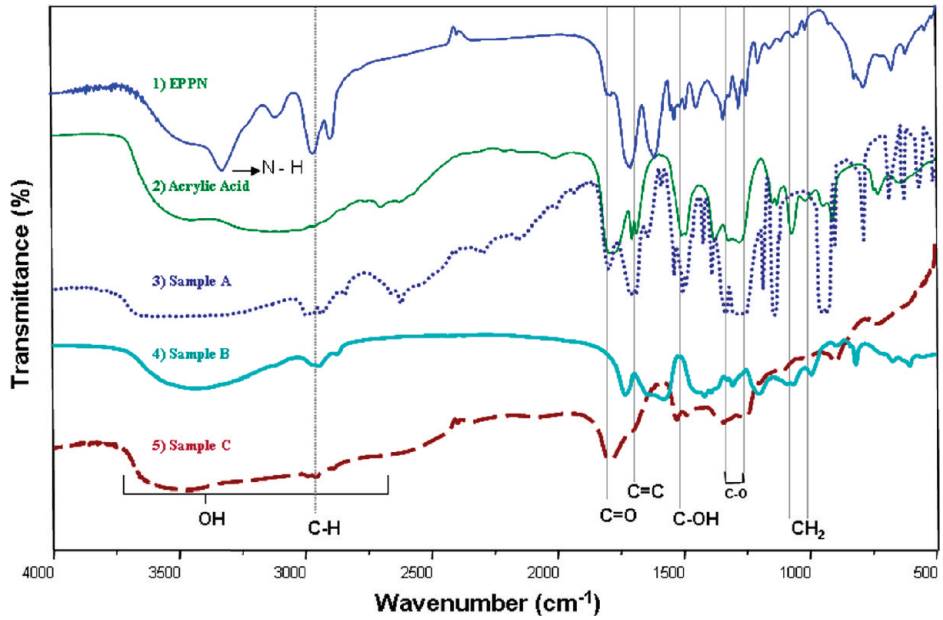

FIGURE 3. FT-IR spectra of (1) EPPN mat, (2) acrylic acid monomer, (3) PAA extracted from the EPPN mat without drying before the start of the extraction process, (4) PAA extracted from the dried EPPN mat at 80 °C in an oven before the start of the extraction process, and (5) polymerized PAA.

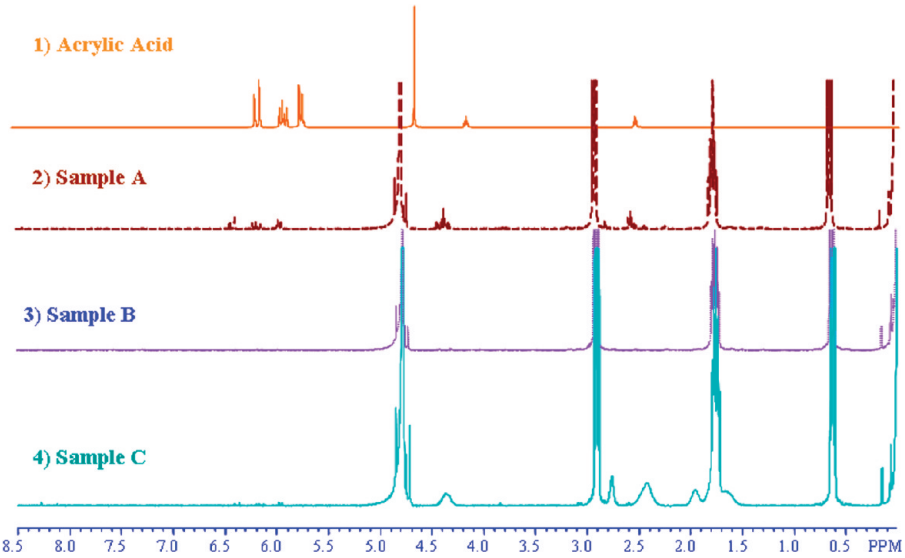

FIGURE 4. ^{1}H NMR spectra of (1) acrylic acid monomer, (2) extracted PAA from the EPPN mat without drying before the extraction process, (3) PAA extracted from the EPPN mat with drying at 80 °C before the start of the extraction process, and (4) polymerized PAA.

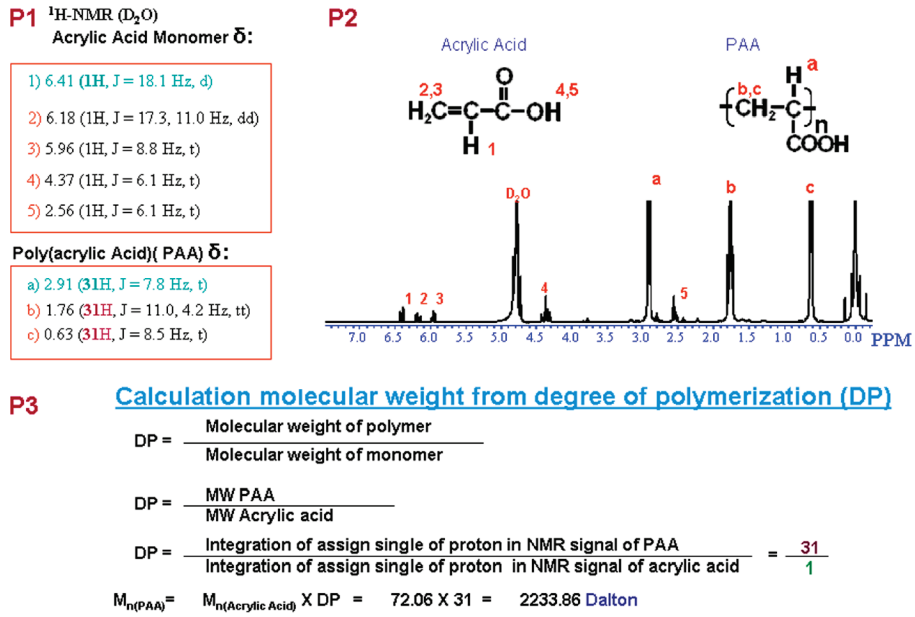

FIGURE 5. Calculation of the molecular weight by reference to ^{1}H NMR peaks: (P1) NMR chemical shifts are separated from Table 1, input 2; (P2) NMR spectrum of sample A, which contains two molecular picks, i.e., acrylic acid and PAA; (P3) calculated molecular weight of PAA by integration of the acrylic acid proton.

Scheme 1. Formic Acid Initiated PAA Polymerization Mechanism

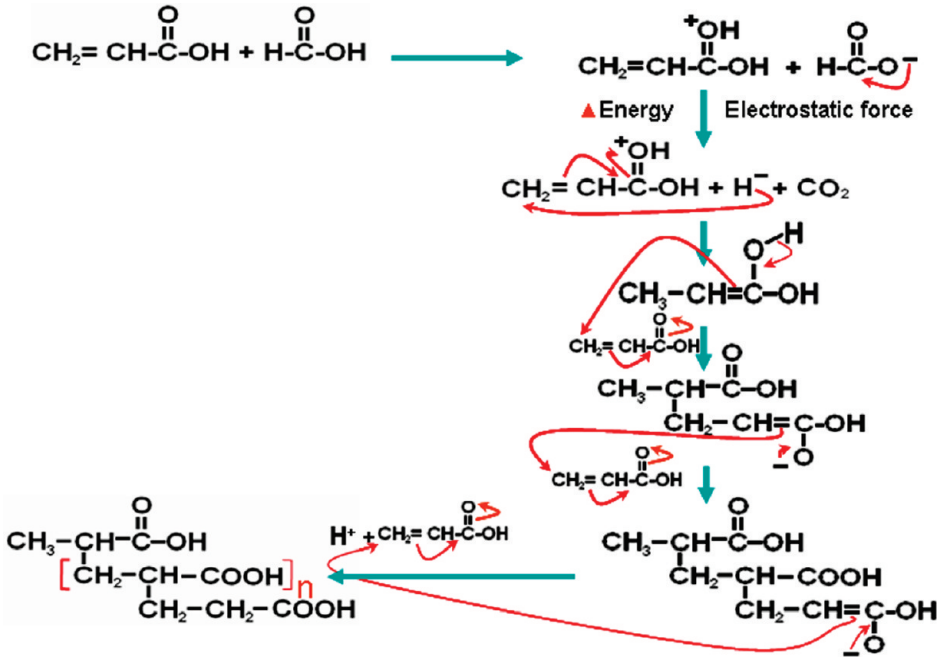

RESULT AND DISCUSSION

In the electrospinning process, an electrified polymeric solution and acrylic acid monomer were extruded through a spinneret by the electrostatic force between two opposite poles. This electric force increases the energy in the reacting substrate to induce a chemical reaction. In this study, these changes were observed via thermogravimetric analysis (TGA) measurement; the EPPN mat was conducted with an Elmer TGA 6 thermogravimetric analyzer (Perkin-Elmer Inc., Waltham, MA) under a nitrogen atmosphere. Approximately 3 mg of sample was heated in a platinum pan from 30 to 800 °C at a rate of 10 °C/min on a differential thermogravimetry (DTG) graph of the fibrous mat as shown in Figure 1B, in which various peaks represent the thermal behavior of material at particular temperatures. The temperature correlation with the maximum thermal degradation rates for nylon 6 and PAA observed in this study is consistent with those reported in the literature. Min et al. reported a maximum thermal degradation rate for nylon 6 at 475 °C, and Lu et al. reported peak maximum thermal degradation rates for PAA250K at 210 and 405 °C (30, 31). Figure 1B reports similar temperatures of maximum thermal degradation rates. The TGA curve shown in Figure 1A indicates that different conjugative mechanisms represent the different components present within the fibrous material.

Furthermore, the hybrid property of the EPPN mat at stable conditions was confirmed by the decrease of the crystalline structure of the nylon 6 mat to the EPPN hybrid mat via an X-ray diffractometer [Rigaku X-ray diffractometer (Rigaku, Japan) with Cu KR (λ) = 1.540 Å radiation over a Bragg angle ranging from 5 to 65°]. X-ray diffraction (XRD) patterns are shown in Figure 2, in which the spectrum of pure nylon 6 is shown as a dotted line. A peak appears at $2\theta = 20.62°$, and this 2θ position is shifted to 19.92° on the XRD pattern; this 0.7 unit decrease defined the nylon 6 along with other components, which must be PAA in EPPN.

The EPPN mat, extracted samples, and polymerization sample were examined with FT-IR spectroscopy separately, and these were performed with KBr pellets using an ABB Bomen MB100 spectrometer (Bomen Inc., St. Laurent, Quebec, Canada). To explain the FT-IR spectrum of the EPPN mat, it is shown in Figure 3(1). The peak at 1645 cm^{-1} corresponds to the stretching mode of the carbonyl moiety of both the amide and keto groups. The peak at 2937 cm^{-1} is attributed to the stretching mode of the CH_2 group, which is important for stability of the polymer chain. The peaks corresponding to the hydrogen-bonding stretching mode of both −OH and $-NH_2$ groups appear between 3137 and 3703 cm^{-1}. The sharply pointed stretching peak at 3309 cm^{-1} is related to the stretching mode of the free N−H bond. Finally, many mixed stretching peaks are observed for different functional groups found in the single hybrid fiber.

EPPN hybrid mats are used to extract samples like samples A and B and characterized separately. Likewise, the chemical functionality of sample A was characterized by FT-IR spectroscopy, shown in Figure 3(3). The peak at 1722 cm^{-1} corresponds to the carbonyl group stretching peak, which shifted from 1713 cm^{-1} in the acrylic acid spectrum shown in Figure 3(2). The wide peaks from 3008 to 3849 cm^{-1} and the peak at 1410 cm^{-1} correspond to hydrogen-bonding and C−OH stretching, respectively. Similarly, stretching peaks corresponding to carbonyl, hydrogen-bonding, and C−OH groups are observed in the spectrum of sample B, shown in Figure 3(4). The two FT-IR spectra in parts (3) and (4) of Figure 2 confirm that samples A and B contain −COOH groups on their backbone. When the FT-IR spectra among the EPPN mat [Figure 3(1)], the extracted solute, and the polymerized sample [Figure 2(3)−(5)] are compared, a free amine stretching peak at 3290 cm^{-1} is observed for nylon 6 of the EPPN mat and is absent in the spectra of samples A−C. This result suggests that the extracted solutes contain carbonyl and hydroxyl groups and hydrogen-bonding −OH bonds on their backbone but do not have free amine bonds. Similarly, the FT-IR spectra of samples B and C indicate that both samples exhibit similar chemical functionality; however, some signals were slightly shifted toward lower frequencies. Further ^{1}H NMR experiments confirmed the equivalence between the extracted and polymerized samples.

^{1}H NMR spectra of the samples and reference compounds were recorded with a JNM-Ex 400 FT-NMR spectrometer (JEOL Ltd., Tokyo, Japan), operating at 400 MHz with a 6% (^{1}H) (w/v) sample solution in D_2O using tetramethylsilane as an internal reference; these are shown in Figure 4. ^{1}H NMR signals at 5.8, 5.9, and 6.2 ppm, present in Figure 4(2), correspond to residual acrylic acid protons in sample A. These signals are similar to those present in the acrylic acid ^{1}H NMR spectrum shown in Figure 4(1), and the remaining peaks are present in the NMR spectrum of sample C. The NMR spectrum of sample B, shown in Figure 4(3), is absent of residual acrylic acid, and the remaining peaks are also equivalent to the NMR spectrum of sample C. The main difference between samples A and B is that sample B was heated at 80 °C for 48 h, which likely caused the volatile acrylic acid monomer to evaporate before polymerization. This result suggests that the electrospun fibrous mat still contains some acrylic acid residue, while the remaining chemical functionality represents the polymerization product. If we compare the NMR spectrum of sample C with those of samples A and B, similar proton singlets are observed at 2.91, 1.76, and 0.63 ppm. It is clear that the arrangements of the NMR peaks for the extracted sample and synthesized polymer are equivalent.

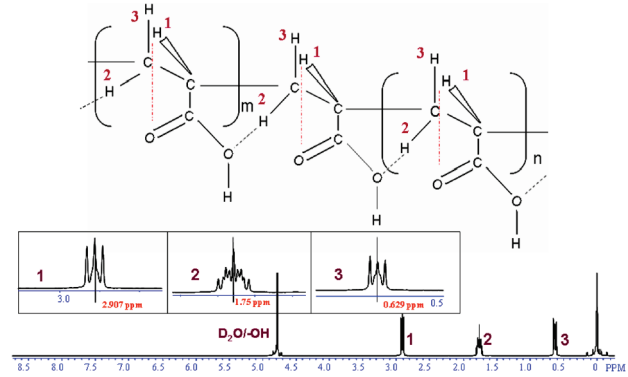

FIGURE 6. Structures of PAA (sample B). Small boxes represent magnifications of the recorded spectrum at its equivalent chemical shift. Numbers are indicated as the equivalent proton of PAA.

Integration of the sample A NMR peaks reveals peaks of different magnitudes, shown in Figure 5. Smaller peaks are assigned to acrylic acid shifts. When the magnitude of the proton is correlated to a bigger one, which is supposed as PAA, we get 31 times less. On the basis of the difference ratio of a polymer like PAA and monomer acrylic acid, the molecular weight of PAA was calculated to be about 2243 Da. If the acrylic acid NMR chemical shift is eliminated in Figure 4(1), the remaining peaks resemble the NMR spectrum of sample B, shown in Figure 4(3). Thus, the NMR spectrum of pure PAA is the same as that of sample B, which is shown in Figure 6.

The FT-IR and ^{1}H NMR spectra show more clearly that the pure extracted PAA has a chemical structure similar to that of sample B. These results also demonstrate that the fibers polymerized via electrospinning contained PAA. It is difficult to fully explain the influence of electricity on the substrate reactivity, a final goal of our attempt chemically to prepare sample C (polymerization product) promising the cause of polymerization via the formic acid hydride ion transfer. This polymerization scheme is illustrated in Scheme 1. Polymerization of acrylic acid occurs through the hydrogen-

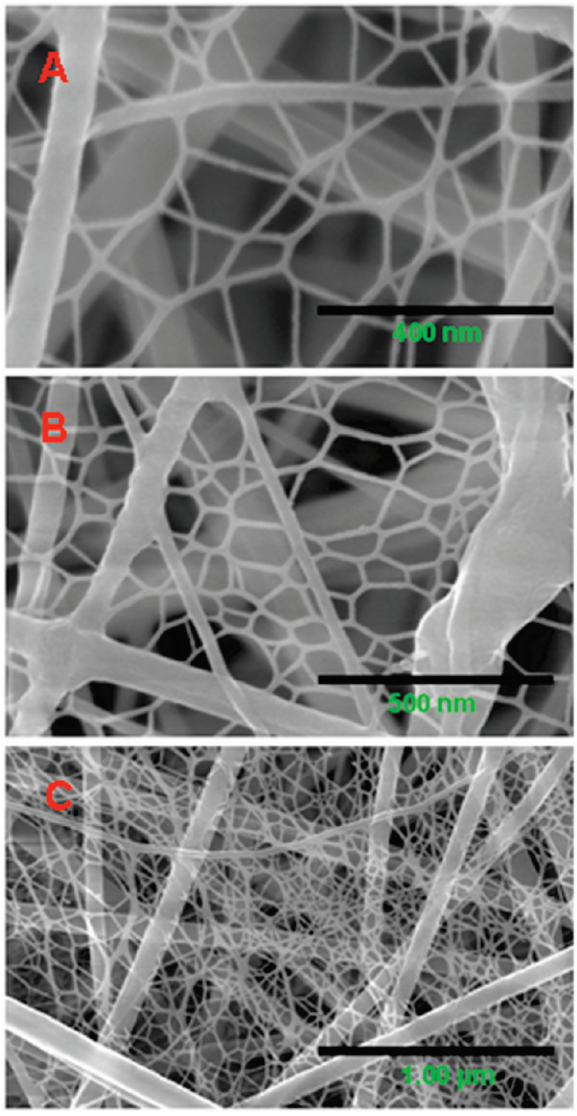

FIGURE 7. FESEM images of the EPPN mat at (A) 130K, (B) 100K, and (C) 50K magnification. Wide areas were covered by interconnected mats in order to show decreasing magnification.

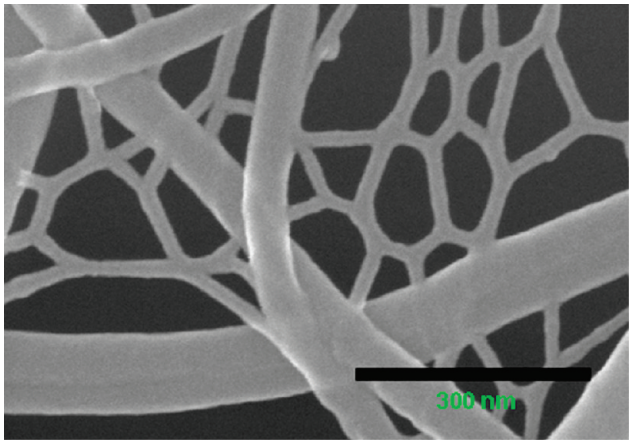

FIGURE 8. FESEM image of the EPPN mat showing a lateral side view of the spider netlike fiber.

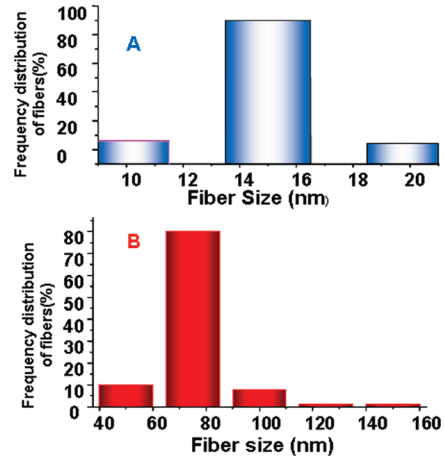

FIGURE 9. Frequency distribution of EPPN fibers in two different ways: (A) a smaller PAA fiber with approximately 15 nm diameter; (B) a bigger nylon 6 fiber having 75 nm diameter.

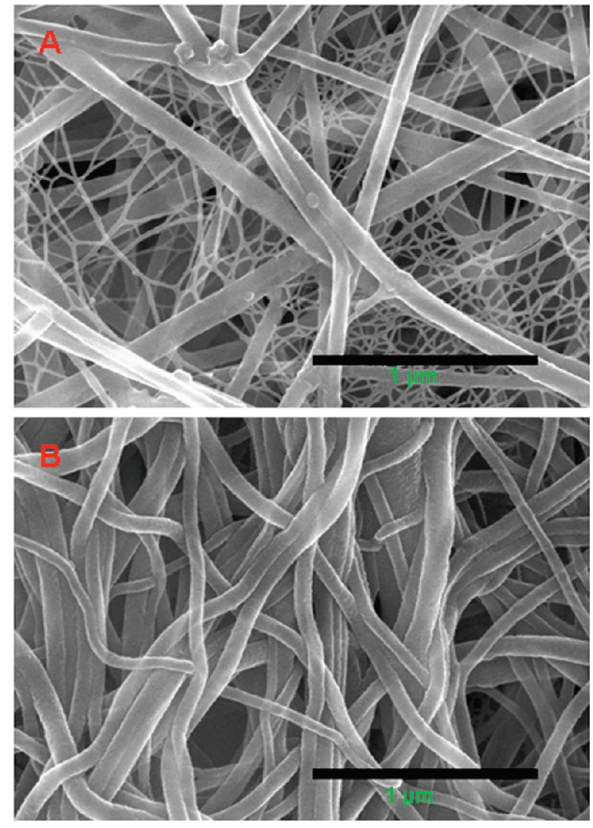

FIGURE 10. FESEM image of the EPPN mat showing (A) interconnected smaller fibers appearing before washing with water and (B) interconnected smaller fiber disappearing after washing with water.

atom-transfer polymerization process. In this process, formic acid acts as a reducing agent, which is activated by the applied voltage. This voltage removes the hydride ion to electrically excite acrylic acid and induce a nucleophilic chain reaction polymerization. This polymerization leads to the formation of a phase-separated polymer layer responsible for a morphological change of the conventional electrospun mat.

During the electrospinning process, when a viscous polymer solution is extruded through the spinneret, a polymer jet is formed because of electrostatic forces (22). The residual charges in this jet begin to repel each other when they become separated from the electrode, causing the fiber

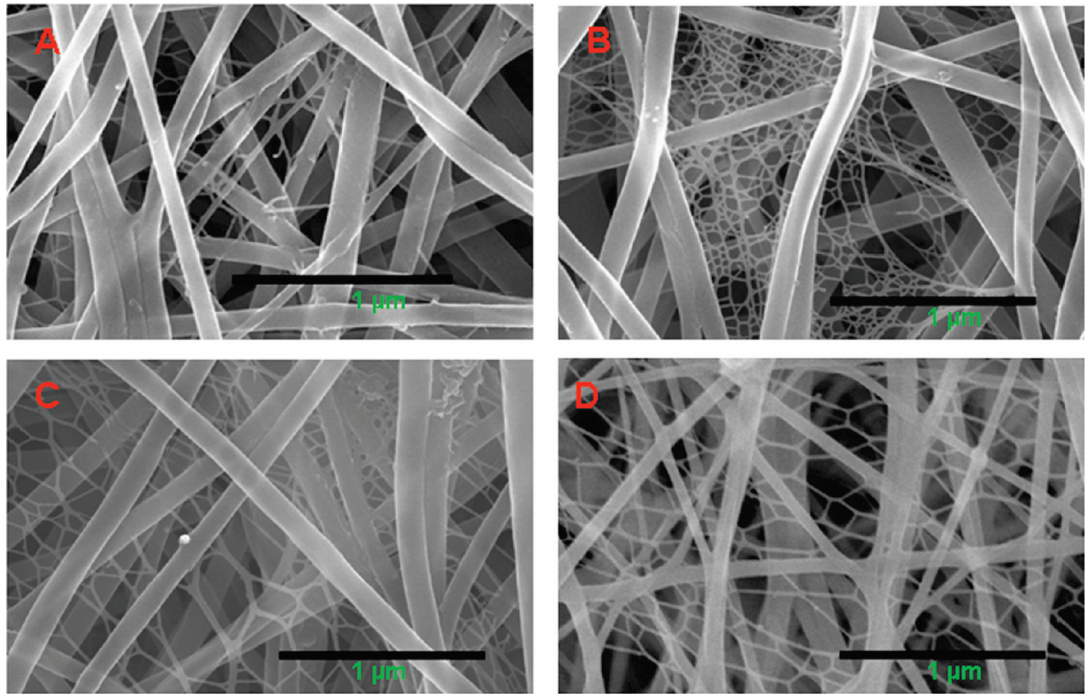

FIGURE 11. FESEM images of EPPN mats with a fixed ratio of a 22 wt % nylon solution, selected as 3 mL, and different ratios of acrylic acid monomer, i.e., (A) 1 mL, (B) 2 mL, (C) 3 mL, and (D) 4 mL.

diameter to grow. Each additional polymer layer becomes cross-linked to form an interconnected fibrous mat. The morphologies of the electrospun mats were examined via field-emission scanning electron microscopy (FESEM; Hitachi Co., Tokyo, Japan) after sputter coating with osmium tetraoxide (OsO_4). These networks appear inside the large fibers shown in Figures 7 and 8. Parts A–C of Figure 7 demonstrate the broad area covered by the fiber network according to a decrease of resolution. Furthermore, a vertical-sectional image of the mat is shown in Figure 8, indicating the lateral side of a similar network surrounding the large fibers with smaller interconnecting fibers. The average fiber diameter is shown in Figure 9, which was recorded based on several FESEM images of fibrous mats. The small fibers had an average diameter of 15 nm, and the large fibers had an average diameter of 75 nm.

Similarly, FESEM images of electrospun mats before and after the extraction process and simply washed or nonwashed electrospun fibrous mats are shown in Figure 10, which demonstrates that the interconnected fibrous mats underwent a change in morphology upon exposure to water, with the large fibers remaining intact. Thus, we can confirm that these large fibers were composed of nylon 6. Hence, the smaller interconnecting fibers must have been composed of PAA, which was destroyed upon exposure to water, as shown in Figure 10B.

Final observations of promoting experiments were taken several times, and different feed ratios of acrylic acid monomer with a fixed viscous nylon solution remarkably enhanced mechanical properties along with the thermal behavior of a nylon 6 and PAA hybrid mat. Research and observation are underway. Here we demonstrated smaller changes exhibited with an increase the volume ratio of acrylic acid, which are shown as Figure 11.

CONCLUSION

Characterization of extracted samples from electrospun mats via FT-IR and NMR spectroscopy revealed carboxylic functional groups and three protons present on each polymer chain. Similarly, investigation of the fiber morphology via FESEM revealed that the PAA fibers (18 nm average diameters) formed a spider netlike arrangement. These smaller nets were water-soluble, suggesting that PAA had been polymerized from acrylic acid monomer in the presence of formic acid in an electrospinning process with the help of a viscous solution. The electric field plays an important role not only in fabrication but also in hydride ion formation from formic acid, which initiated polymerization during the electrospinning process.

Acknowledgment. This research was supported by a Korean Ministry of Education, Science and Technology grant (The Regional Core Research Program/Center for Healthcare Technology Development, Chonbuk National University, Jeonju 561-756, Republic of Korea).

REFERENCES AND NOTES

(1) He, C. H.; Gong, J. *Polym. Degrad. Stab.* **2003**, *81*, 117.
(2) Kim, S. C.; Gong, J.; Lee, D. B.; Lee, D.; Park, S. *Mater. Lett.* **2003**, *57*, 579.
(3) Boland, E. D.; Coleman, B.; Coleman, D. *Acta Biomater.* **2005**, *1*, 115.
(4) Kim, H.; Lee, H. J. *Biomed. Mater. Res.* **2006**, *A79*, 643.
(5) Eugene, D. B.; Gary, E. W.; Simposon, D. G. *J. Macromol.* **2001**, *2*, 231.
(6) Acatay, K.; Simsek, E.; Yang, O. C.; Menceloglu, Y. A. *Angew. Chem., Int. Ed.* **2004**, *43*, 5210.
(7) ML, M.; Hill, R.; Lowery, J.; Fridrikh, S.; Rutledge, G. *Langmuir* **2005**, *21*, 5549.
(8) Liu, H.; Kameoka, J.; Czaplewski, D.; Craighead, H. *Nano Lett.* **2004**, *4*, 671.
(9) Wang, X.; Kim, Y.; Drew, C.; Ku, B. C.; Kumar, J.; Samuelson, L. *Nano Lett.* **2003**, *4*, 331.

(10) Kim, C. H.; Kim, D. S.; Kang, S. Y.; Marquez, M. *Polymer* **2006**, *47*, 5097.
(11) Ding, B.; Li, C.; Miyauchi, Y.; Kuwaki, O.; Shiratori, S. *Nanotechnology* **2006**, *17*, 3685.
(12) Heumann, S.; Ebrrl, A.; Fischer-Colbrie, G.; Pobeheim, H.; Kaufmann, F.; Ribitsch, D.; Cavaco-Paulo, A.; Guebitzl, G. M. *Biotechnol. Bioeng.* **2009**, *102*, 1003.
(13) Elliott, J. E.; Macdonald, M.; Nie, J. *Polymer* **2004**, *45*, 1503.
(14) Budtova, T.; Navard, P. *Macromolecules* **1996**, *29*, 3931.
(15) Zong, Y.; Shan, X.; Watkins, J. *Langmuir* **2004**, *20*, 9210.
(16) Satyabrata, S.; Atanu, K. *Chem. Mater.* **2004**, *16*, 3489.
(17) Bonapasta, A.; Buda, F. *Chem. Mater.* **2001**, *13*, 64.
(18) Wang, X.; Bohn, P. W. *J. Am. Chem. Soc.* **2004**, *126*, 6825.
(19) Sheeney-Haj-Ichia, L.; Cheglakov, Z. *J. Phys. Chem. B* **2004**, *108*, 11.
(20) Tatoulian, M.; Arefi-Khonsari, F.; Tatoulian, L.; Amouroux, J. *Chem. Mater.* **2006**, *18*, 5860.
(21) Taylor, G. *Proc. R. Soc. London* **1969**, *A313*, 1515.
(22) Yu, J. H.; Fridrikh, S. V.; Rutledge, G. C. *Polymer* **2006**, *47*, 4789.
(23) Eustache, F.; Dalko, P. I.; Cossy, J. *Org. Lett.* **2002**, *4*, 1263.
(24) King, R. B.; Bhattacharyya, K. *Sci. Technol.* **1997**, *31*, 984.
(25) Matharu, D. S.; Morris, D. J. *Org. Lett.* **2005**, *7*, 5489.
(26) Uematsu, N.; Fujii, A.; Hashiguchi, S.; Ikariya, T.; Noyori, R. *J. Am. Chem. Soc.* **1996**, *118*, 4916.
(27) Miller, J. I.; Jenkins, A. D.; Tsartolla, E.; Joseph, M. I. *Polym. Bull.* **1988**, *20*, 247.
(28) Allen, R. O.; Long, T. E.; McGrath, J. E. *Polym. Bull.* **1886**, *15*, 127.
(29) Pugh, C.; Percec, V. *Polym. Bull.* **1985**, *14*, 109.
(30) Min, W.; Walter, D.; Brad, U.; Yanqiu, S.; Francis, E. P.; Wang, X.; White, J. L.; Balik, C. M.; Rusa, C. C.; Fox, J.; Tonelli, A. E. *Macromolecules* **2002**, *35*, 8039.
(31) Lu, X.; Yang Tan, C. Y.; Xu, J.; He, C. *Synth. Met.* **2003**, *138*, 429.

AM800191M